



**INSTITUTE OF  
ENERGY CONVERSION**

University of Delaware  
Newark, De 19716-3820  
Ph: 302/831-6200  
Fax: 302/831-6226  
www.udel.edu/iec

---

**UNITED STATES DEPARTMENT OF ENERGY  
UNIVERSITY CENTER OF EXCELLENCE  
FOR PHOTOVOLTAIC RESEARCH AND EDUCATION**

October 25, 2007

Bolko von Roedern  
National Renewable Energy Laboratory  
1617 Cole Boulevard  
Golden, CO 80401

Re: NREL Subcontract #ADJ-1-30630-12  
D.5.23

Dear Bolko,

This report covers research conducted at the Institute of Energy Conversion (IEC) for the period of September 1, 2007 to September 30, 2007, under the subject subcontract. The report highlights progress and results obtained under Task 1 (CdTe-based solar cells).

**Task 1 - CdTe-based Solar Cells**

**Summary**

This report presents results obtained for research under Task 1, CdTe-based solar cells. During this period, effort was focused on methods for improving module performance and fabrication of devices with thin CdTe absorber layers.

**Improving Module Performance**

In thin film superstrate CdTe devices, CdS is the optimal heteropartner to obtain good junction performance. However, the CdS contributes negligible current to the total output and a fraction of the CdS film is lost during cell processing due to diffusion into the CdTe absorber layer; the precise quantity varies from 10-40 nm depending on the CdTe grain size distribution, deposition temperature and post-deposition treatment temperature-time conditions. The high degree of coupling between the CdS thickness and  $V_{OC}$  requires careful control of CdS thickness during the CdTe deposition and post-deposition processing. For high throughput processing of large area devices needed for modules, obtaining optimal performance and uniformity would

furthermore require critical control of temperature uniformity and time. A poorly understood aspect of window layer processing for CdTe cells is the relationship between the CdS surface chemistry and electronic properties that can affect the junction. In particular, the role of native oxides on CdS, the effect of impurities from soda-lime glass on CdS and the electronic state of the CdS film is neither understood nor controlled. These issues are being addressed by characterizing the CdS surface chemistry using x-ray photoemission spectroscopy (XPS) and the electronic state by surface photovoltage analysis.

#### *Factors affecting CdS surface photovoltage*

The surface photovoltage of CdS films was characterized by measuring the open-circuit voltage obtained with liquid junctions using aqueous quinhydrone (pH = 3.5) and polysulfide (pH = 12) electrolytes with platinum electrodes. The redox potentials of these electrolytes are favorable for comparative diagnostics of CdS electronic properties and surface states. The redox potentials of the quinhydrone and polysulfide solutions were 5.15 V and 4.91 V, respectively, with respect to vacuum level. Measurements were made using 0.02 cc drops of electrolyte applied to the CdS surface followed by insertion of a Pt wire. The device configuration was illuminated with an ELH tungsten filament lamp at 80 mW/cm<sup>2</sup>. CdS films deposited by different techniques were compared in as-deposited conditions with the two electrolytes (Table I). The deposition methods evaluated were chemical surface deposition (CSD) at 55°C, physical vapor deposition (PVD) at 200°C, and close space sublimation (CSS) at 600°C. All films were deposited at IEC using ACS grade CdSO<sub>4</sub> and thiourea for CSD films and GE high purity CdS powder (6N purity) for PVD and CSS films.

Table I. Surface photovoltage of as-deposited CdS films fabricated by different methods onto Ga<sub>2</sub>O<sub>3</sub>/SnO<sub>2</sub>/SLG substrates.

Sample	Deposition Method	Temperature (°C)	V <sub>oc</sub> Quinhydrone (mV)	V <sub>oc</sub> Polysulfide (mV)
P175	CSD	55	-300	-400
41242	PVD	200	-505	-750
CdS001	CSS	600	-550	-650

In Table I, higher surface photovoltage was obtained with polysulfide electrolyte than with quinhydrone, in part due to the higher redox potential of the former, which allows for a greater built-in potential for junctions with CdS. The measured potential difference (typically 100 mV) is less than the redox potential difference of the electrolytes (260 mV), indicating different flat-band potentials for these electrolytes in contact with CdS. The surprising difference is the nearly consistent increase in surface photovoltage obtained at progressively higher deposition temperatures. While the results for the CSD films in polysulfide electrolyte are consistent with those reported for CdS single crystal in similar solution<sup>1,2</sup>, the evaporated films yielded significantly higher photovoltages, which is consistent with a shift on the CdS Fermi level towards the conduction band, i.e., greater n-type conductivity, or a reduction in the density of surface states. We will continue to employ this simple technique as a tool for correlating changes in CdS processing with surface chemistry and performance of CdTe/CdS solar cells.

### *CdS Surface chemistry*

The surface composition of single crystal CdS and thin film CdS deposited by chemical surface deposition (CSD) was measured by x-ray photoemission spectroscopy (XPS) using a Physical Electronics system with Al x-ray source. As shown in Table II, the single crystal and CSD thin film compositions are very similar (Table II first two rows) with the atomic concentration ratio of Cd/S close to unity. Physically adsorbed carbon comprises about 20% of the surface and slightly lower oxygen quantity was detected. For the sulfur component peaks at 168.997eV (Figure 1 crystal CdS) and 169.077eV (Figure 2 thin film CdS) are found on each specimen. The positions of the peaks show that part of the sulfur is bound as sulfate, likely due to native oxides formed on the surfaces of both crystal and thin film CdS during storage. The atomic concentration ratio of sulfur in sulfate state to oxygen is about 1:5.

After 10 minutes of Ar<sup>+</sup> ion milling of the single crystal CdS surface, oxygen and carbon signals decreased and the Cd/S ratio did not change. For the sulfur, the peak around 169 eV disappeared, indicating removal of sulfate below the crystal surface. The etching of thin film CdS produced similar results, and we determined the thin film CdS etch rate in Ar<sup>+</sup> to be about 4-5 nm per minute. However, after etching 30 seconds, the carbon signal on the thin film CdS reduced to the detection limit.

Table II. CdS single crystal and thin film surface composition determined by XPS.

CdS Samples	Cd (3d5/2)		S (2p3/2)		O (1s)		C (1s)	
	Position (eV)	At. Con.	Position (eV)	At. Con.	Position (eV)	At. Con.	Position (eV)	At. Con.
		(%)		(%)		(%)		(%)
Crystal (surface)	405.495	31.4	161.791 (168.997)	31.3	532.019	13.8	285	23.5
Thin film (surface)	405.724	31.2	161.964 (169.077)	31.0	532.359	17.7	285	21.1
Crystal (10 min etching)	405.000	41.0	161.319	40.3	531.462	4.3	285	14.4
Thin film (30 sec etching)	405.564	47.9	161.826	46.0	531.725	6.1	No Carbon	0
Thin film (60 sec etching)	405.481	49.2	161.744	48.7	531.867	2.1	No Carbon	0

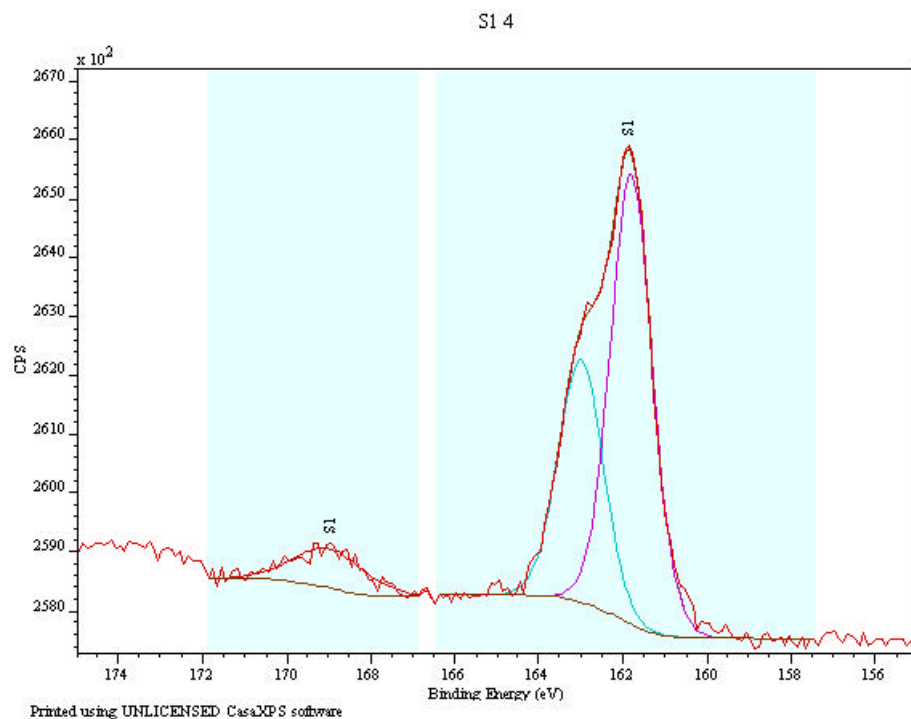


Figure 1. Sulfur on crystal CdS surface before etching. Shading indicates peak fitting region for compositional analysis.

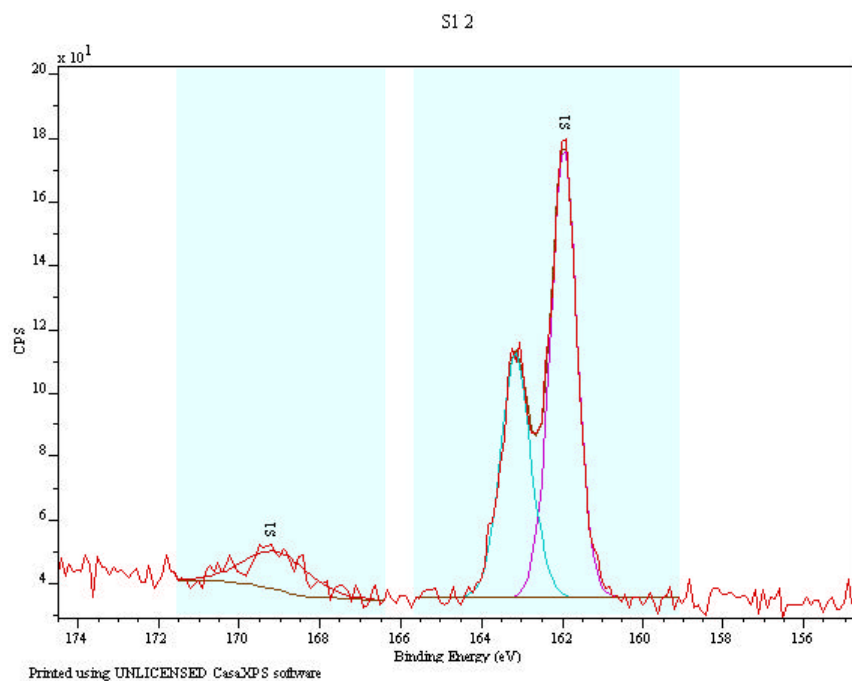


Figure 2. Sulfur on thin film CdS surface before etching. Shading indicates peak fitting region for compositional analysis.

Two thin film samples deposited by CSD were analyzed by glancing incidence x-ray diffraction (GIXRD) to determine the crystalline phase content of the near-surface region for different processing methods. Samples were deposited with single and double concentrations of  $\text{NH}_4\text{OH}$  in otherwise similar solutions at  $55^\circ\text{C}$ . Both samples exhibited similar patterns, with a surface phase of  $\text{CdSO}_4$ .

Two identically deposited CdS films (single ammonia concentration) were then treated and analyzed: One sample was immersed in acetic acid at temperature  $60^\circ\text{C}$  for 10 minutes, while the other sample was heat treated in the air at temperature at  $450^\circ\text{C}$  for two hours. Then both samples were analyzed by GIXRD within 10 minutes following each treatment, with the measurement taking 60 minutes. While the purpose of acetic acid treatment was removal of  $\text{CdSO}_4$ , the GIXRD results showed no difference with respect to before treatment, indicating either that acetic acid did not remove any oxides on the surface, or the oxide formation is so rapid that no difference can be detected by XRD, since XRD analysis took one hour to finish. The heat treatment should to increase surface oxidation, and the GIXRD results exhibit three additional peaks, corresponding to  $\text{Cd}_3\text{O}_2\text{SO}_4$  and  $\text{CdSO}_3$ . In addition, recrystallization of CdS film was detected. From XPS results discussed above, the ratio of sulfur in sulfate state to oxygen is about 1:5. Therefore, it seems likely that both  $\text{CdSO}_4$  and  $\text{Cd}_3\text{O}_2\text{SO}_4$  phases may exist on the surface of the CdS thin film samples. The GIXRD data also suggests that a small quantity of  $\text{CdSO}_3$  resides on the surface too; the particular oxides phases may form on different terminating surfaces of the CdS allowing oxides with different stoichiometry to form in addition to the widely cited stable  $\text{CdSO}_4$  phase. Further information about  $\text{Cd}_3\text{O}_2\text{SO}_4$  and  $\text{CdSO}_3$  is needed to determine the stability of this compound and if it can exist on the surface of CdS.

GIXRD analysis of CSD CdS films deposited in the standard bath and then treated with  $\text{CdCl}_2$  in air ambient at  $450^\circ\text{C}$  for 20 minutes also shows:  $\text{Cd}_3\text{O}_2\text{SO}_4$ ,  $\text{CdSO}_4$  and  $\text{CdSO}_3$  phases before treatment and additional  $\text{Cd}_3\text{O}_2\text{SO}_4$  after the treatment. Thus, for annealing with  $\text{CdCl}_2$ , additional oxides form on the surface. Experiments were conducted to try to modify the phase content of the surface using vapor anneal treatments.

Two fresh CSD CdS film samples were treated in 4% hydrogen-argon at temperature  $500^\circ\text{C}$  for 30 minutes to attempt to remove oxides from the surface. Calculation shows that the diffusion of O into bulk CdS is about  $1.8 \times 10^{-3} \text{ \AA}$  per hour. The GIXRD analysis duration is about 50 minutes, so CdS bulk should be slightly oxidized during the analysis. The first sample (718-15) was analyzed by GIXRD immediately following the hydrogen treatment, while the other sample (314-4) was stored in argon for 1 hour. The GIXRD analysis for both samples shows that two peaks corresponding to  $\text{Cd}_3\text{O}_2\text{SO}_4$  were indeed reduced. Together with the results after heat treatment, we can see that the oxidation of CdS and reduction both occur in the form of oxide  $\text{Cd}_3\text{O}_2\text{SO}_4$ . Thus, the problem now is controlling  $\text{CdSO}_4$  and  $\text{CdSO}_3$ . Two CSD CdS films after  $\text{CdCl}_2$  heat treatment were treated in hydrogen-argon at  $600^\circ\text{C}$  for 60 minutes, with the result that both  $\text{CdSO}_3$  and  $\text{Cd}_3\text{O}_2\text{SO}_4$  were significantly removed from the GIXRD pattern. We plan to evaluate the surface photovoltage and the performance of VT CdTe/CdS devices using CdS films with different surface conditions and oxide content.

## Process Development for Cells with Thin CdTe Absorber

The IEC VT deposition process is being used to deposit CdTe films with thickness approaching 1 micron suitable for cells with 11% conversion efficiency. However, the thickness uniformity of the obtained deposit is more difficult to control in the high deposition rate regime (10  $\mu\text{m}/\text{min}$ ) than for baseline thickness  $\sim 5\text{--}7\ \mu\text{m}$ . Also, the films are more prone to having voids in the CdTe layer, which become shunt paths in devices. The post-deposition processing becomes more critical since thinner films have smaller grains and are therefore more sensitive to grain boundary-enhanced processes such as interdiffusion of CdS-CdTe, oxide penetration, and penetration from any etchants used to process the back contact. In the previous year of work, we showed that 11% baseline performance could be maintained with 1.5-3 micron thick CdTe by reducing the  $\text{CdCl}_2$  vapor treatment processing time, using milder etchants, and reducing the Cu quantity at the back contact, either by depositing a thinner layer or by incorporating the Cu into the ZnTe contact. Bifacial spectral response (SR) and capacitance voltage (C-V) analysis of CdTe devices with optimized performance at different CdTe thickness allowed the depletion width  $W$  and diffusion length  $L$  to be evaluated. The values for  $W$  and  $L$  deduced from  $\text{SR}_B$  analysis and  $W$  values measured by C-V are shown in Table III. There is excellent agreement for  $W$  from SR and C-V measurements for devices with different absorber thicknesses.

Table III.  $W(V)$  obtained from  $\text{SR}_B$  analysis and C-V measurements for cells with ZnTe:Cu contacts, different CdTe thickness and having 11% conversion efficiency.

Sample	Thickness ( $\mu\text{m}$ )	$L(\mu\text{m})$	$W(\mu\text{m})$			
			@ (-1.0V)		@ (0V)	
			SR	CV	SR	CV
B	8	0.76	5.5	5.4	4.8	4.8
C1	5	0.72	2.6	2.4	2.4	2.0
D	3	0.6	1.8	1.7	1.3	1.4

This data shows that the depletion width in optimized cells is approximately half the CdTe thickness, which is a result of the combined processing changes of reducing the  $\text{CdCl}_2$  vapor treatment time, using a milder etch, and reducing the Cu quantity. This is the starting point for experiments using devices with VT deposited CdTe with 1 micron film thickness. VT CdTe depositions were carried out at a growth rate of  $\sim 6$  microns/minute at a substrate temperature of  $525^\circ\text{C}$  onto  $\text{CdS}/\text{Ga}_2\text{O}_3/\text{SnO}_2/\text{SLG}$  (TEC-15). The  $\text{CdCl}_2$  treatment was carried out with the CdTe sample at  $480^\circ\text{C}$  and the  $\text{CdCl}_2$  source at  $425^\circ\text{C}$  for 1 minute. A dilute hydrazine solution was used to remove oxides and form a thin Te layer. The back contact was fabricated by deposition of 2 nm Cu, reaction at  $180^\circ\text{C}$  to form  $\text{Cu}_2\text{Te}$  and application of graphite paste. The best cells obtained had AM1.5 conversion efficiencies up to 7%, typified by low  $V_{\text{OC}}$  but good photocurrent and complete consumption of the CdS film, as shown in the J-V and QE plots below. In this device, the low  $V_{\text{OC}}$  and FF are undoubtedly related to the loss of CdS, with the primary junction now between the  $\text{CdTe}_{1-x}\text{S}_x$  absorber and the  $\text{Ga}_2\text{O}_3/\text{SnO}_2$  buffer layer. The QE data shows good photogeneration with the 1 micron absorber layer and relatively flat response from 550 to 820 nm. Effort is on-going to optimize the post-deposition treatment and evaluate the effect of CdS thickness and buffer layer properties.

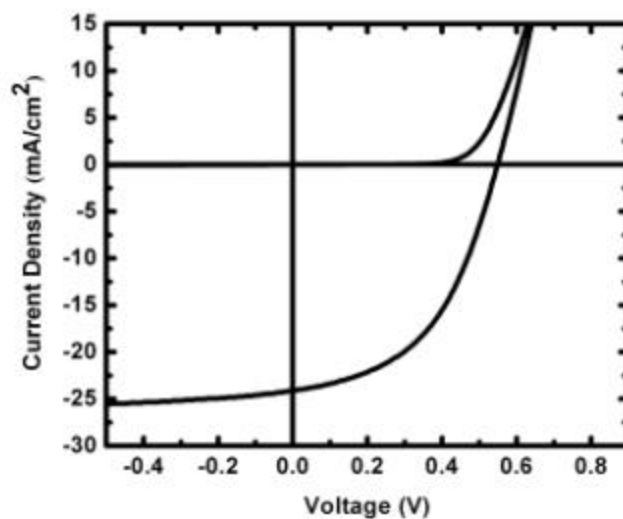


**Figure 3. J-V plot of light and dark behavior of VT CdTe/CSD CdS sample VT279.1 with 1 micron thick absorber layer processed with vapor CdCl<sub>2</sub> and Cu/C contact.**

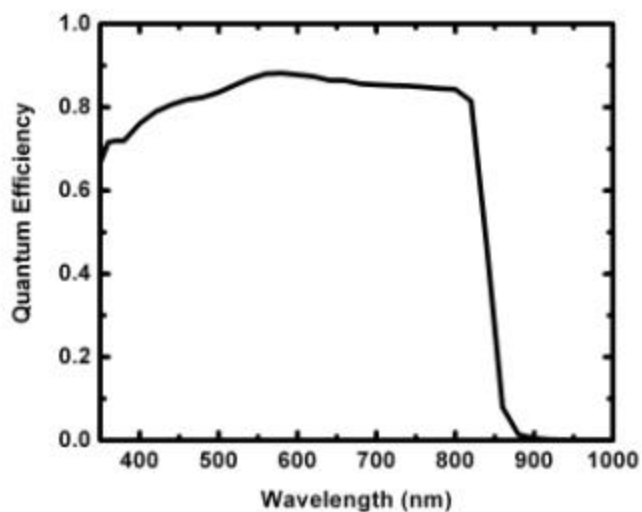


**Figure 4. QE versus wavelength of VT CdTe/CSD CdS sample VT279.1 with 1 micron thick absorber layer processed with vapor CdCl<sub>2</sub> and Cu/C contact.**

Best regards,

Robert W. Birkmire  
Director

CC: Paula Newton, IEC  
Susan Tompkins, RGS  
Carolyn Lopez, NREL

References:

---

- 1 A. B. Ellis, S. W. Kaiser, M. S. Wrighton, J. Amer. Chem. Soc. **98** (22), 6855 (1976).
- 2 H. Harada, T. Ueda, T. Sakata, J. Phys. Chem. **93**, 1542 (1989).